arXiv:1612.06450v1 [physics.plasm-ph] 19 Dec 2016

Plasma Wave Seed for Raman Amplifiers

Kenan Qu, Ido Barth, and Nathaniel J. Fisch
Department of Astrophysical Sciences, Princeton University, Princeton, New Jersey 08544, USA
(Dated: December 21, 2016)

It is proposed to replace the traditional counter-propagating laser seed in backward Raman amplifiers with a plasma wave seed. In the linear regime, namely for constant pump amplitude, a plasma wave seed may be found by construction that strictly produces the same output pulse as does a counter-propagating laser seed. In the nonlinear regime, or pump-depletion regime, the plasma-wave initiated output pulse can be shown numerically to approach the same self-similar attractor solution for the corresponding laser seed. In addition, chirping the plasma wave wavelength can produce the same beneficial effects as chirping the seed wave frequency. This methodology is attractive because it avoids issues in preparing and synchronizing a frequency-shifted laser seed.

PACS numbers: 52.35.Mw, 52.59.Ye, 42.65.Yj

To overcome the thermal damage limit of conventional materials [1, 2], it has been proposed to employ plasma to mediate intense laser amplification [3, 4]. Different backscattering coupling techniques were then explored, including Compton scattering [3, 5], resonant Raman scattering [4, 6–12], Brillouin scattering [13–17], and chirped pump Raman amplification [18]. In a Raman amplifier, a long pump laser pulse deposits its energy to a counterpropagating, short, amplified pulse mediated by a plasma wave. The amplified pulse duration contracts while its amplitude grows, thereby producing an ultra-intense laser pulse. To initiate the amplification, the amplified pulse is seeded by a short laser seed, down-shifted from the pump frequency by the plasma frequency, and synchronized to meet the pump as the pump leaves the plasma. Preparing such a frequency-shifted, synchronized laser seed represents a significant technological challenge.

It has been proposed for strongly-coupled Brillouin scattering to form a laser seed by reflection of the pump [19]. However, a simple reflection does not produce the frequency downshift necessary for Raman resonance. It is proposed here instead to replace the laser seed with a plasma wave seed. The plasma wave has negligible group velocity, so without regard for synchronization, the amplification process is triggered only when the pump wave reaches it. In Fig. 1, we compare seeding by a laser pulse (a) and by a plasma wave (b). For laser seeding, there exist solutions in which an intense counter-propagating wave is produced, with pump depletion (c), in which the counter-propagating pulse consumes essentially all the energy of the pump beam, while contracting in time [4]. These solutions give rise to extreme intensities. However, there are other solutions, depending on how the laser seed is prepared with a front that is not steep enough, or with not enough initial energy content, in which these promising solutions do not obtain [20]. The question to be answered here is whether one can construct with a plasma wave seed the same promising solutions that were constructed with a suitably constructed laser seed.

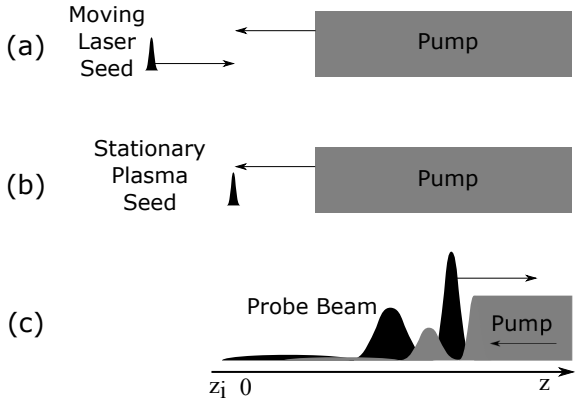

FIG. 1. Seeding of the amplified output pulse. The pump laser is applied from the right direction. (a) Triggered by a counter-propagating laser seed. (b) Triggered by a stationary plasma wave seed. (c) In the case of an advantageous result, the amplified output pulse assumes a π-pulse shape accompanied by depletion of the pump laser.

What is shown here is that, in fact, such solutions for the counter-propagating pulse, which we shall call the "probe pulse", can be constructed for the plasma wave seed as well, and that they are attractor solutions. For nearly all laser-seeded interactions resulting in complete pump depletion, a plasma-wave-seeded interaction can be found to produce the same time-asymptotic output pulse. This reachable subset includes the advantageous output pulses depicted in Fig. 1(c). Moreover, we show that the advantages that accrue to laser seeding through frequency chirping [21] can be realized as well through plasma wave seeding with wavelength chirping.

To proceed, consider the three-wave resonant Raman coupling process [22]. For the case of the seeded plasma wave, an electron density ripple is produced, δn, with a wavevector $\vec{k}_f$. This ripple is produced in only a small localized region at the far end of the plasma, at the end where the pump wave exits. When encountered by the incident pump laser with a wavevector $\vec{k}_a$, electrons oscillate at velocity $\vec{v}$, and hence induce a transverse current

$\vec{j} = -e\vec{v}\delta n$ with a wavevector $\vec{k}_b = \vec{k}_a - \vec{k}_f$, where e is the elementary charge. If the wavevector and frequency of the transverse current $\vec{j}$ are properly matched, a probe beam is generated. Importantly, for efficient Raman amplification, the dispersion relation determines the choice of $\vec{k}_f$ such that $(\omega_a - \omega_f)^2 = \omega_p^2 + c^2(\vec{k}_a - \vec{k}_f)^2$, where ω_a is the pump frequency and $\omega_f = \sqrt{\omega_p^2 + 3v_{\rm th}^2 k_f^2}$ is the plasma seed frequency. Here, ω_p and $v_{\rm th}$ are the plasma frequency and the electron thermal velocity, respectively. For cold and underdense plasmas, $\omega_f \approx \omega_p \ll \omega_a$; hence, $k_f \approx 2k_a$. Note that in the case of the laser seed, the frequency ω_b is red detuned from the pump frequency by ω_f. In contrast, the plasma wave seed should have the appropriate wavelength, and then the appropriately red-tuned frequency probe is automatically generated.

To develop an equivalence rule between laser and plasma seeds, we make the reasonable assumption that similar linear solutions (constant pump amplitude) will transition to the same nonlinear asymptotic attractor solutions which feature pump depletion. This assumption, of course, must be checked. However, the linearization allows us to rigorously construct a plasma wave seed with Green's function response identical to that of a laser seed that has the desired wavefront sharpness and intensity.

Consider the configuration as illustrated in Fig. 1(b). At $t = 0$, the pump coming from the right edge meets the Langmuir wave at $z = 0$. We describe the envelopes of the pump and probe lasers using the wave vector potentials a and b, normalized such that the pump power density is $I_a = 2c\varepsilon_0(\pi m_e c^2|a|/e\lambda_a)^2 = 1.37\times10^{18}(a/\lambda_a[\mu\mathrm{m}])^2[\mathrm{W\,cm^{-2}}]$, and similarly for I_b; f is the envelope of Langmuir wave normalized to $Vf = (e/m_e c)|E_e|$, where $V \approx \sqrt{\omega_a\omega_p}/2$ for underdense plasmas (*i.e.*, $\omega_a \approx \omega_b \gg \omega_p$) and linearly polarized optical beams. Without losing generality, we assume real a and keep b and f complex. Here m_e is the electron mass; E_e is the electrostatic field of the Langmuir wave; c is the speed of light; and ε_0 is the permittivity of free space. For simplicity, we neglect, at this stage, the group velocity dispersion (GVD), relativistic nonlinearity, and kinetic effects. The resonant three-wave equations in cold plasma can then be written as [4]

$$a_t - ca_z = -Vbf, \quad b_t + cb_z = Vaf^*, \quad f_t = Vab^*, \tag{1}$$

where the subscriptions t and z denote the partial time and z derivatives, respectively.

In the linear stage, before the pump beam gets depleted (*i.e.*, a remains constant), the solution to Eqs. (1) can be obtained [23] for $b(t,z) = b_{\rm f}(t,z) + b_{\rm b}(t,z)$, where

$$b_{\rm f}(t,z) = \int {\rm d}z' G_{\rm bf}(t, z-z') f_0(z'), \tag{2}$$

$$b_{\rm b}(t,z) = \int {\rm d}z' G_{\rm bb}(t, z-z') b_0(z'), \tag{3}$$

are the components of the probe generated by a plasma seed $f_0(z)$ and a laser seed $b_0(z)$, respectively, and

$$G_{\rm bf}(t,z) = \frac{\gamma_0}{c} I_0(\xi)\cdot\Theta(t-\frac{z}{c}), \tag{4}$$

$$G_{\rm bb}(t,z) = \frac{1}{\gamma_0}\frac{\partial}{\partial t}G_{\rm bf}(t,z) = \frac{\gamma_0}{c}\sqrt{\frac{z}{ct-z}} I_1(\xi)\cdot\Theta(t-\frac{z}{c}) + \frac{1}{c}\delta(t-\frac{z}{c}), \tag{5}$$

are the Green's functions associated with the corresponding seeds [24]. Here $I_0(\cdot)$ is the zeroth order modified Bessel function, $\Theta(\cdot)$ is the Heaviside function, $\gamma_0 = a_0 V$ denotes the linear temporal growth rate, and $\xi = 2(\gamma_0/c)\sqrt{z(ct-z)}$.

In laser-seeded amplification, $f_0 = 0$ and $b_0 \neq 0$. The probe beam comprises the initial laser seed [the second term in Eq. (5)] and the generated components from three-wave process [the first term in Eq. (5)]. The generated component grows quasi-exponentially and hence eventually dominates the probe. For a given laser seed, $b_0(z)$, we now look for a plasma seed, $f_0(z)$, such that the resulting probe (in the linear regime) is the same, *i.e.*, $b_{\rm f}(t,z) = b_{\rm b}(t,z)$.

First, in analyzing the Green's functions, note that

$$\frac{c}{\gamma_0}\frac{\partial}{\partial z}G_{\rm bf}(t,z) = -G_{\rm bb}(t,z) + \frac{\gamma_0}{c}\sqrt{\frac{ct-z}{z}} I_1(\xi)\cdot\Theta(t-\frac{z}{c}), \tag{6}$$

where the last term can be neglected at the wavefront $z - ct \ll z$. The identity (6) suggests taking the envelope of plasma wave seed to be

$$f_0(z) = \frac{c}{\gamma_0}\frac{\partial}{\partial z} b_0(z), \tag{7}$$

so that the generated probe beam can be found using integration by parts

$$\begin{aligned} b_{\rm f}(t,z) &= \int {\rm d}z' G_{\rm bf}(t, z-z')\frac{c}{\gamma_0}\frac{\partial}{\partial z'} b_0(z') \\ &= -\int {\rm d}z' b_0(z')\frac{c}{\gamma_0}\frac{\partial}{\partial z'} G_{\rm bf}(t, z-z') \\ &\cong \int {\rm d}z' G_{\rm bb}(t, z-z') b_0(z'). \end{aligned} \tag{8}$$

Comparing Eqs. (3) and (8) shows that the plasma wave seed, initiated according to Eq. (7), generates asymptotically a probe beam that has the identical wavefront which is generated by use of a laser seed.

As the probe pulse propagates and grows, if initially short enough, it should eventually deplete the pump and enter into the nonlinear or so-called "π-pulse" regime, characterized by the self-similar contracting pulse envelope [4]. The asymptotic equivalence expressed by Eq. (7) suggests that asymptotically identical pulses in the linear regime should evolve to identical pulses in the nonlinear

regime. In the limit of short (delta function) laser seeds, and correspondingly short plasma seeds, a formal equivalence can be made [23]. While the finite width case does not follow rigorously, we show numerically that the equivalence in fact does extend to finite pulse widths.

Thus, for finite width seeds, by numerically solving Eqs. (1), we compare amplification triggered by a plasma seed to that by a laser seed. As shown in Fig. 2(a), the laser seed envelope is Gaussian with $b_0(z) = 0.03a_0 \exp[-(1+\gamma_0 z/c)^2/\sigma^2]$ with normalized width $\sigma = 0.5$. Following the equivalence rule in Eq. (7), the plasma seed is taken as $f_0(z) = (c/\gamma_0)\partial b_0(z)/\partial z$. The two peaks in f_0 differ by a phase difference of π. In Fig. 2(b), we observe, at $\gamma_0 t = 1$, that the probe beam generated by the plasma seed has a wavefront that exactly matches the laser seed. The identical wavefronts generated by different seeds ensure the same Raman amplification throughout $\gamma_0 t = 40$, as shown in Fig. 2(b)-(e). They both reveal similar π-pulse structures, with the amplitude in its leading peak increasing linearly and the pulse duration similarly contracting linearly in distance.

While we have constructed an envelope of the plasma seed that approaches the corresponding attractor solution of the laser seed, it is not necessarily a unique correspondence. Note that, while the laser seed has but one, the plasma seed in Fig. 2(a) has two maxima, or two humps. But the asymptotic solution clearly depends on only the first hump, since the pump interaction with that hump will clearly shadow the second hump. Indeed, removing the second hump will give the identical asymptotic solution, which in practice makes easier the setting up of the plasma wave seed.

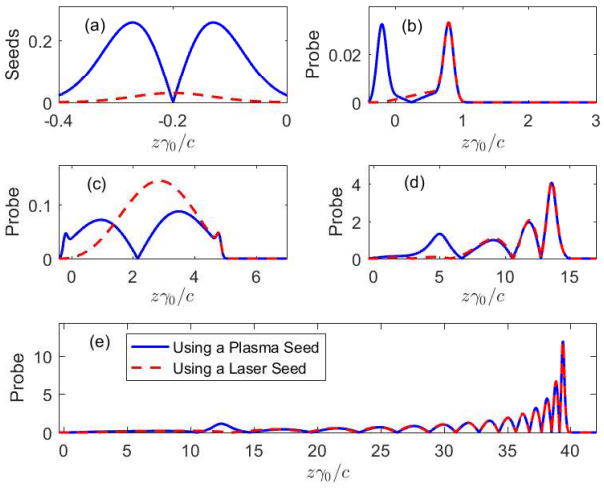

FIG. 2. (Color online). (a) Envelopes of plasma seed (blue solid line) and laser seed (red dashed line). (b)-(e) Amplified probe pulse at times $\gamma_0 t = 1, 5, 15$, and 40. Blue solid lines correspond to plasma seed; red dashed lines to laser seed.

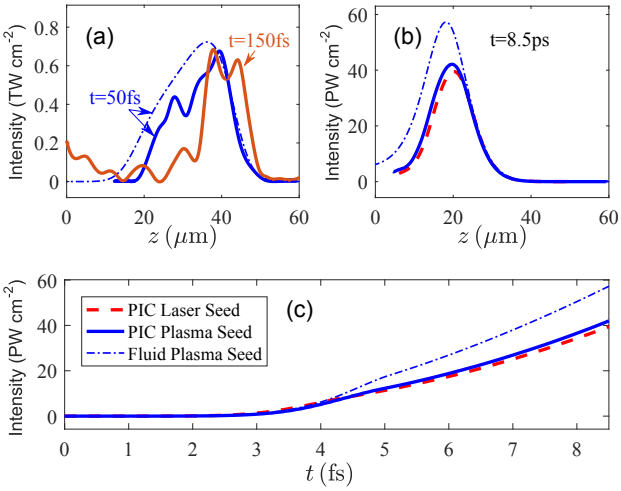

FIG. 3. (Color online). (a) Amplified probe pulse using a plasma seed at different interaction times. (b) Leading spike of amplified probe pulses using a plasma seed (blue solid line) and a laser seed (red dashed line). (c) Comparison of the amplified probe pulse peak intensity. The thick solid and dashed lines are PIC simulations; and the thin dotted-dash lines are fluid-model simulations using Eqs.(1).

To compare kinetic effects using laser and plasma seeds, we conducted one-dimensional particle-in-cell (PIC) simulations (using the code EPOCH [25]). For definiteness, we considered parameters similar to those of recent experiments [7, 11]. The electron density is $n_e = 1.5 \times 10^{19}\text{cm}^{-3}$ and accordingly $\omega_p = 2\pi \times 35\,\text{THz}$. The pump laser has wavelength $\lambda_a = 0.8\,\mu\text{m}$ and intensity $I_a = 0.4\,\text{PW}\,\text{cm}^{-2}$. The linear growth rate is $\gamma_0 = 5\,\text{ps}^{-1}$. The low temperature (10 eV) suppresses Landau damping. A cell size of 4 nm is used to match the Debye length, with 800 electrons per cell to reduce charge density fluctuations. Calculations are done in a $60\,\mu$m window moving with the group velocity of the probe ($v_g = 0.9948c$).

The simulation results are shown in Fig. 3. The simulation includes, in addition to kinetic effects, effects such as group velocity dispersion and relativistic nonlinearity, neglected in the hydrodynamic analysis. The laser seed is Gaussian with width $10\,\mu\text{m} \approx 0.16c/\gamma_0$, and peak intensity $0.8\,\text{TW}\,\text{cm}^{-2}$. Its frequency is set at $\omega_b = 2\pi \times 340\,\text{THz}$, obeying the frequency matching. For the plasma wave seed, as discussed, the double peak structure with a π-phase difference may be eschewed in favor of a single peak. Thus, we use a Gaussian to approximate the leading peak, with a normalized width $7.1\,\mu\text{m} \approx 0.117\,c/\gamma_0$, while ignoring the second peak. The amplitude of the electrostatic seed wave is $5 \times 10^9\,\text{V/m}$, which is associated with a 50% electron density oscillation. Its wavelength is $0.4\,\mu$m, so that $k_p = 2k_a$.

Note that, immediately after the interaction, a probe

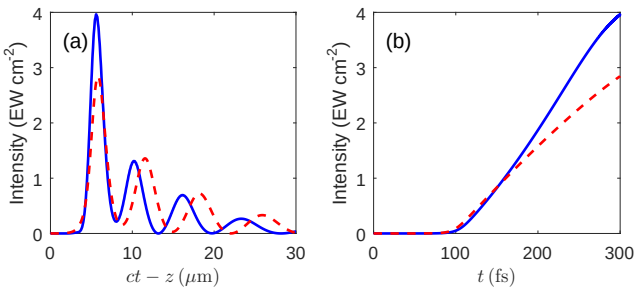

FIG. 4. (Color online). (a) Amplified probe beams triggered by chirped (blue solid) and non-chirped (red dashed) plasma seeds with a 300 fs pump pulse; (b) growth of the peak intensities. The seed amplitudes and shapes are identical.

beam is generated [see Fig. 3(a)]. Its wavefront increases in sharpness. For comparison, we also show the numerical solution of Eq. (1) as dashed lines. The comparison indicates that the plasma seed indeed triggers the Raman amplification like a laser seed does. No precursors are observed, but the moving window would suppress those. In Fig. 3(c), which shows the growth of the peak intensity, we identify the linear stage amplification (before $\sim$ 4.5ps), exhibiting an intensity exponentially increasing in time (or distance) and the nonlinear stage (after $\sim$ 4.5ps), exhibiting a quadratically increasing intensity. After an amplification time of 8.5 ps, the leading spikes of the probes shown in Fig. 3(b) both reach 40 PW cm^{-2}, which is 100 times higher than the pump intensity. The pump depletion at the probe peak is 75% for both seeds. The agreement between the PIC simulations with plasma and laser seeds is very good for both the leading peak envelopes [Fig. 3(b)] and the maximum intensity [Fig. 3(c)]. They also decently match the numerical solutions of Eq. (1), although PIC simulations show asymptotically lower peak intensities. The discrepancy might be due to kinetic effects that are taken into account in PIC, but not in the fluid model, or due to the envelope approximation in the fluid model.

For higher plasma density where group velocity dispersion (GVD) becomes important, one can advantageously chirp the laser seed to reduce the required plasma length [21]. Since higher frequency components propagate faster, the front of the chirped probe sharpens due to GVD. It is of interest to inquire whether the same advantages can accrue for a plasma wave seed. In fact, for plasma seeds, the advantageous chirping effects can be accomplished by chirping the wavelength of the plasma wave, such that the generated probe is also chirped.

To show this, we first modify Eq. (1) by including the GVD term for the probe [21]

$$b_t + c_b b_z = Vaf^* + i\kappa b_{tt}, \tag{9}$$

where $\kappa = (1/2c_b)(\partial c_b/\partial\omega_b) = \omega_p^2/(2c_b\omega_b)$ and c_b is the group velocity of the seed. In Fig. 4, we compare amplification in a high density plasma with a chirped plasma seed to amplification with a non-chirped plasma seed. The parameters are chosen similar to those in Ref. [21], *i.e.*, $n_e = 12\times10^{20}$cm^{-3}, $\lambda_a = 0.351\,\mu$m, $I_a = 12.2\,$PW cm^{-2} and the plasma length is 90 μm. The plasma seeds are both Gaussian with FWHM of 1.8 μm. The nonchirped seed has a uniform wavevector $k_f = k_a + k_b = 2\pi/0.215\,\mu$m. The output intensity reaches 2.8 EW cm^{-2}. Here, the wavevector, k_f, of the chirped plasma seed increased 3.5% per μm, where pump interacts with lower k_f first. Since the pump has a constant frequency, the generated probe is also chirped with smaller wavenumbers (smaller frequencies) at the front. Due to GVD, the probe contracts when traveling through the plasma. Similar to the case of a chirped laser seed [21], the probe beam has a larger growth rate and its intensity reaches 4 EW cm^{-2}. From Fig. 4(a), we also observe an appropriately narrower probe pulse.

Can any laser seed be replaced by an equivalent plasma wave seed? Clearly, for a seed laser pulse envelope that is not differentiable, the formal equivalent plasma seed envelope does not exist. However, this restriction on shape is not important, since the seed laser pulse need be no more sharp than a Maxwellian in order to access the π-pulse, pump depletion regime [20], for which equivalent plasma seeds do exist. More relevant is the restriction on the amplitude; while a seed laser pulse envelope can take an arbitrarily large amplitude, the Langmuir wave seed amplitude will be limited by the wavebreaking limit. In a cold plasma, this condition is equivalent to a maximum density variation $\delta n < n_0$; in a warm plasma the density variation is somewhat more limited [26, 27]. However, this will not be an issue in the main amplification regimes [28] for which the necessary laser seeding amplitudes can be small [29]. Also, even a small plasma wave seed can access operation near the wave breaking limit [30, 31], since that limit is determined by the pump amplitude, not the seed amplitude. The density restriction may be an issue though in the so-called *quasi-transient* regime, where damping of the Langmuir wave is significant, so amplification is achieved only with larger laser seed amplitudes [32]. The corresponding amplitudes may then not be available for plasma wave seeds. However, these regimes are in any event not of interest for plasma wave seeding, since, if the plasma wave is heavily damped, the advantage of synchronization is absent.

In summary, a Langmuir wave seed can, in principal, replace almost any useful laser seed in backward Raman amplifiers, generating a probe beam that has an identical wavefront. The method can also be generalized by using a chirped plasma wave wavelength to mimic the frequency chirping of a laser seed. These predictions are supported by by hydrodynamic and fully kinetic 1D-PIC simulations. The promise of this method is that it represents an alternative technology in implementing compression of high intensity lasers in plasma, with a particular

advantage concerning the timing of the pulses.

Although the technological production of the plasma wave seed is beyond the scope of this work, the ability of plasma wave seeds to linger in plasma has been utilized in suggestions both for plasma holography [33] and plasma photonic crystals [34]. Also, plasma wave seeds might be manipulated through autoresonant techniques to achieve the desirable properties [35]. The prescription for Langmuir wave seed offered here can be generalized to other types of plasma waves with negligible group velocity that might mediate high intensity laser compression in plasma, such as, for example, the ion acoustic wave for compression by stimulated Brillouin scattering.

This work was supported by NNSA Grant No. DE-NA0002948, and AFOSR Grant No. FA9550-15-1-0391.

[1] D. Strickland and G. Mourou, "Compression of amplified chirped optical pulses," Opt. Commun. **56**, 219–221 (1985).

[2] A. Dubietis, G. Jonušauskas, and A. Piskarskas, "Powerful femtosecond pulse generation by chirped and stretched pulse parametric amplification in BBO crystal," Opt. Commun. **88**, 437 – 440 (1992).

[3] G. Shvets, N. J. Fisch, A. Pukhov, and J. Meyer-ter-Vehn, "Superradiant amplification of an ultrashort laser pulse in a plasma by a counterpropagating pump," Phys. Rev. Lett. **81**, 4879–4882 (1998).

[4] V. M. Malkin, G. Shvets, and N. J. Fisch, "Fast compression of laser beams to highly overcritical powers," Phys. Rev. Lett. **82**, 4448–4451 (1999).

[5] M. Dreher, E. Takahashi, J. Meyer-ter-Vehn, and K.-J. Witte, "Observation of superradiant amplification of ultrashort laser pulses in a plasma," Phys. Rev. Lett. **93**, 095001 (2004).

[6] Y. Ping, W. Cheng, S. Suckewer, D. S. Clark, and N. J. Fisch, "Amplification of ultrashort laser pulses by a resonant Raman scheme in a gas-jet plasma," Phys. Rev. Lett. **92**, 175007 (2004).

[7] W. Cheng, Y. Avitzour, Y. Ping, S. Suckewer, N. J. Fisch, M. S. Hur, and J. S. Wurtele, "Reaching the nonlinear regime of Raman amplification of ultrashort laser pulses," Phys. Rev. Lett. **94**, 045003 (2005).

[8] J. Ren, S. Li, A. Morozov, S. Suckewer, N. A. Yampolsky, V. M. Malkin, and N. J. Fisch, "A compact double-pass raman backscattering amplifier/compressor," Phys. Plasmas **15**, 056702 (2008).

[9] N. A. Yampolsky and N. J. Fisch, "Current limiting effects on laser compression by resonant backward Raman scattering," Phys. Plasmas **18**, 056711 (2011).

[10] C.-H. Pai, M.-W. Lin, L.-C. Ha, S.-T. Huang, Y.-C. Tsou, H.-H. Chu, J.-Y. Lin, J. Wang, and S.-Y. Chen, "Backward Raman amplification in a plasma waveguide," Phys. Rev. Lett. **101**, 065005 (2008).

[11] Y. Ping, R. K. Kirkwood, T.-L. Wang, D. S. Clark, S. C. Wilks, N. Meezan, R. L. Berger, J. Wurtele, N. J. Fisch, V. M. Malkin, E. J. Valeo, S. F. Martins, and C. Joshi, "Development of a nanosecond-laser-pumped Raman amplifier for short laser pulses in plasma," Phys. Plasmas **16**, 123113 (2009).

[12] G. Lehmann and K. H. Spatschek, "Non-filamentated ultra-intense and ultra-short pulse fronts in three-dimensional Raman seed amplification," Phys. Plasmas **21**, 053101 (2014).

[13] A. A. Andreev, C. Riconda, V. T. Tikhonchuk, and S. Weber, "Short light pulse amplification and compression by stimulated Brillouin scattering in plasmas in the strong coupling regime," Phys. Plasmas **13**, 053110 (2006).

[14] L. Lancia, J.-R. Marquès, M. Nakatsutsumi, C. Riconda, S. Weber, S. Hüller, A. Mančić, P. Antici, V. T. Tikhonchuk, A. Héron, P. Audebert, and J. Fuchs, "Experimental evidence of short light pulse amplification using strong-coupling stimulated Brillouin scattering in the pump depletion regime," Phys. Rev. Lett. **104**, 025001 (2010).

[15] S. Weber, C. Riconda, L. Lancia, J.-R. Marquès, G. A. Mourou, and J. Fuchs, "Amplification of ultrashort laser pulses by Brillouin backscattering in plasmas," Phys. Rev. Lett. **111**, 055004 (2013).

[16] L. Lancia, A. Giribono, L. Vassura, M. Chiaramello, C. Riconda, S. Weber, A. Castan, A. Chatelain, A. Frank, T. Gangolf, M. N. Quinn, J. Fuchs, and J.-R. Marquès, "Signatures of the self-similar regime of strongly coupled stimulated Brillouin scattering for efficient short laser pulse amplification," Phys. Rev. Lett. **116**, 075001 (2016).

[17] M. R. Edwards, N. J. Fisch, and J. M. Mikhailova, "Strongly enhanced stimulated Brillouin backscattering in an electron-positron plasma," Phys. Rev. Lett. **116**, 015004 (2016).

[18] B. Ersfeld and D. A. Jaroszynski, "Superradiant linear Raman amplification in plasma using a chirped pump pulse," Phys. Rev. Lett. **95**, 165002 (2005).

[19] H. Peng, Z. H. Wu, Y. L. Zuo, Z. M. Zhang, K. N. Zhou, and J. Q. Su, "Single laser pulse compression via strongly coupled stimulated Brillouin scattering in plasma," Phys. Plasmas **23**, 073516 (2016).

[20] Yu. A. Tsidulko, V. M. Malkin, and N. J. Fisch, "Suppression of superluminous precursors in high-power backward Raman amplifiers," Phys. Rev. Lett. **88**, 235004 (2002).

[21] Z. Toroker, V. M. Malkin, and N. J. Fisch, "Seed laser chirping for enhanced backward Raman amplification in plasmas," Phys. Rev. Lett. **109**, 085003 (2012).

[22] W. L Kruer, *The physics of laser plasma interactions* (Reading, MA (US); Addison-Wesley Publishing Co., 1988).

[23] See Supplemental Material for the derivation.

[24] G. Shvets and J. S. Wurtele, "Free electron lasers 1996 SASE in plasmas: Analysis and simulation of Raman backscatter from noise," Nucl. Instrum. Meth. A **393**, 371 (1997).

[25] T. D. Arber, K. Bennett, C. S. Brady, A. Lawrence-Douglas, M. G. Ramsay, N. J. Sircombe, P. Gillies, R. G. Evans, H. Schmitz, A. R. Bell, *et al.*, "Contemporary particle-in-cell approach to laser-plasma modelling," Plasma Phy. Contr. F. **57**, 113001 (2015).

[26] T. P. Coffey, "Breaking of large amplitude plasma oscillations," Physics of Fluids (1958-1988) **14**, 1402–1406 (1971).

[27] A. Bergmann and H. Schnabl, "The influence of electron trapping on stationary langmuir waves,"

Phys. Plasmas **31**, 3266–3270 (1988).
[28] D. S. Clark and N. J. Fisch, "Operating regime for a backward Raman laser amplifier in preformed plasma," Phys. Plasmas **8**, 3363 (2003).
[29] N. A. Yampolsky, V. M. Malkin, and N. J. Fisch, "Finite-duration seeding effects in powerful backward Raman amplifiers," Phys. Rev. E **69**, 036401 (2004).
[30] M. R. Edwards, Z. Toroker, J. M. Mikhailova, and N. J. Fisch, "The efficiency of Raman amplification in the wavebreaking regime," Phys. Plasmas **22**, 074501 (2015).
[31] Z. Toroker, V. M. Malkin, and N. J. Fisch, "Backward Raman amplification in the langmuir wavebreaking regime," Phys. Plasmas **21**, 113110 (2014).
[32] V. M. Malkin and N. J. Fisch, "Quasitransient regimes of backward Raman amplification of intense x-ray pulses," Phys. Rev. E **80**, 046409 (2009).
[33] I. Y. Dodin and N. J. Fisch, "Storing, retrieving, and processing optical information by Raman backscattering in plasmas," Phys. Rev. Lett. **88**, 165001 (2002).
[34] G. Lehmann and K. H. Spatschek, "Transient plasma photonic crystals for high-power lasers," Phys. Rev. Lett. **116**, 225002 (2016).
[35] I. Barth, I. Y. Dodin, and N. J. Fisch, "Ladder climbing and autoresonant acceleration of plasma waves," Phys. Rev. Lett. **115**, 075001 (2015).